Contents

2. Testing of Typical Spacecraft Materials in a Simulated Substorm Environment

N. John Stevens, Frank D. Berkopec, John V. Staskus,
Richard A. Blech, and Steven J. Narciso
National Aeronautics and Space Administration
Lewis Research Center
Cleveland, Ohio

Abstract

A series of survey tests have been conducted in the Lewis Research Center
substorm simulation facility. The test specimens were spacecraft paints,
silvered Teflon, thermal blankets and solar array segments. The samples, rang-
ing in size from 300 to 1000 cm^2 were exposed to monoenergetic electron energies
from 2 to 20 keV at a current density of 1 nA/cm^2. The samples generally behaved
as capacitors with strong voltage gradients at their edges. The charging charac-
teristics of the silvered Teflon, Kapton, and solar cell covers were controlled by
the secondary emission characteristics. Insulators that did not discharge were
the spacecraft paints and the quartz fiber cloth thermal blanket sample. All other
samples did experience discharges when the surface voltage reached -8 to -16 kV.
The discharges were photographed. The breakdown voltage for each sample was
determined and the average energy lost in the discharge was computed.

1. INTRODUCTION

Many satellites in geosynchronous orbits have experienced and are experiencing anomalous behavior in their electronic systems at various times in their operational life. [1,2] This behavior is believed to be caused by the environment charging the insulator surfaces to the point that discharges can occur. [3] These discharges will produce an electromagnetic pulse which can couple into the spacecraft harness and cause an anomaly. Since parts of the satellite that are shaded can charge to a different value from a sunlit surface, the discharge can be between a shaded insulator and the spacecraft structure. Therefore, in order to understand this charging phenomenon, it is necessary to know how typical spacecraft materials respond to the charging environment and to determine what factors influence this charging.

An investigation to determine the materials characteristics under the charging conditions has been initiated at the NASA-Lewis Research Center under the joint USAF-NASA interdependency program. [4] This investigation is a continuation of the work initiated to support the Canadian-American Communications Technology Satellite program. [5]

The approach used in the materials characterization testing was to expose selected test specimens to simulated substorm conditions and determine their response to these conditions. The specimen surface potential and the specimen leakage current to ground were measured as a function of the simulation conditions. From this data the charge deposited and the energy stored in the sample were computed. For those tests where discharges occurred, the surface potential at breakdown, the charge lost and the energy dissipated in the discharge were determined. These tests were run on simple samples to investigate the material characteristics as a function of material geometry, thickness, surface temperature and test duration. Additional tests were run on more complex samples to determine the effects of assembly techniques, surroundings, and multiple surfaces on samples.

This paper will describe the results of survey-type testing conducted on the typical spacecraft external coatings listed in Table 1. The survey-type test is basically a short duration test of 20 minutes at each beam voltage. This period is sufficient to insure that the sample surface has come to its equilibrium potential. The tests were run in the Lewis geomagnetic substorm simulation facility. [6] The test results reported here are for 1 nA/cm^2 beam current density tests. Unless otherwise specified all data is for dark conditions with the sample at room temperature. More detailed test reports on the samples can be found in the literature. [7-9]

Table 1. LeRC Materials Characterization Studies

Materials tested
Spacecraft paints
S-13G nonconductive paint
Conductive paints
Silvered Teflon samples
Thermal blanket samples
Kapton outer layer
Quartz cloth outer layer
Solar array segments
Standard cells on fiberglass substrate
Solar cells on flexible substrate
Solar cells with conductive film coverglass

2. PROCEDURE

The typical data set for the testing is shown in Figure 1. A capacitively coupled, noncontacting surface voltage probe is used to verify that the initial surface potential was zero and then swept across the test surface at fixed time intervals after the sample charging started. Since the probe functions with the beam operating, there is no need to interrupt the test to obtain the surface potential data. This procedure is followed for the test duration and results in transient charging curves for each test conditions. Each time the probe is swept across the sample, voltage profiles are automatically obtained. The typical steady-state profiles for insulating films are shown in the figure.
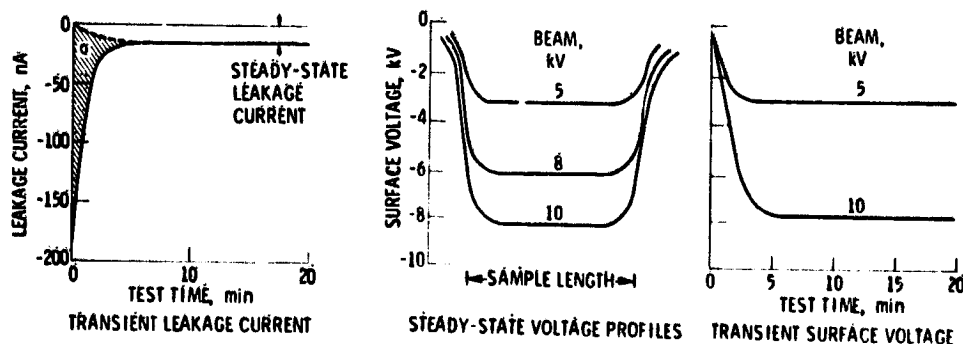

Figure 1. Typical Data Set of Materials Characterization Tests

The total leakage electron current to ground is measured as a function of time after the test start. A typical example of the electron current flow to ground is also shown in Figure 1. This current shows the characteristics of capacitor charging; an initial surge decaying with time to a steady-state value. The charge deposited on the surface can be obtained by integrating this transient current (as shown by the shaded area). Once the charge and surface potential are known, the capacitance and energy storage can be computed. The steady-state values of the surface potential and leakage current can be used to compute the effective resistance of the sample.

The same type of data can be used to obtain the discharge characteristics for the samples that experienced discharges. The voltage probe is used to follow the surface voltage through the discharge. In this manner the breakdown voltage and the potential of the surface after discharge can be determined. The transient leakage current is used to determine the charge deposited up to the breakdown and the charge remaining after the discharge. From this data the charge lost and the energy dissipated in the discharge can be computed.

3. TEST RESULTS

3.1 Spacecraft Paints

3.1.1 SAMPLE DESCRIPTION

Both conductive and nonconductive paint samples have been tested. The nonconductive paint chosen for evaluation was the S-13G low outgassing white paint. This paint uses zinc oxide as the pigment with an RTV silicone as the vehicle. The sample dimensions were 17 by 20 cm by 0.02 cm thick.

The conductive paints were black, white, and yellow conductive paints supplied by the Goddard Space Flight Center. These paints were formulated with conductive pigment to provide desired optical properties. The sample area was also 340 cm^2 but the thickness was 0.01 cm.

3.1.2 TEST RESULTS

The results of the simulation test are shown in Figure 2. The conductive paints did not charge; the surface potential remained less than 1 V for all beam voltage conditions. There was no apparent physical damage to the samples as a result of these tests. It is planned to conduct long duration tests of these samples to determine if there will be any time dependent degradation due to the electron bombardment.
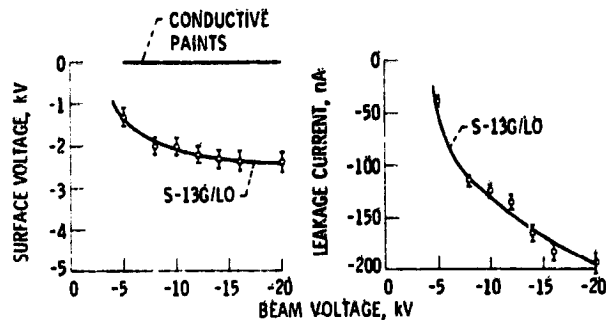
Figure 2. Spacecraft Paints Charging Survey Data

The nonconductive paint does charge but soon reaches a limiting value of about -2200 V. The behavior is typical of those insulators whose resistance decreases with voltage. The steady-state leakage current values verify this resistance decrease. There were no visible discharges during these tests nor was there any apparent damage to the samples as a result of the tests. It was noted, however, that the sample did "electrofluoresce" under electron bombardment — it glowed in the beam.

3.2 Silvered Teflon Samples

3.2.1 SAMPLE DESCRIPTION

All of the tests described in this section were conducted with 15 by 20 cm silvered Teflon samples, 0.013 cm (5 mil) thick, with the Teflon surface exposed to the electron flux. The sample was usually made by covering a grounded metal substrate with 5 cm wide strips of silvered Teflon tape. A conductive adhesive was used so that the silver layer was electrically grounded within a few ohms.

3.2.2 TEST RESULTS

3.2.2.1 Charging Characteristics

The results of these tests are shown in Figure 3. The steady-state surface voltage profiles (a) show that the central portion of the insulator reaches a uniform potential dependent only on the beam voltage. Therefore, the central portion of the insulator seems to acquire the characteristics of a conductor — no transverse electric field. However, there is a very pronounced edge voltage gradient that appears to become more pronounced with increasing beam voltage. Apparently these edge voltage gradients can drive currents around the edges contributing significantly to the total leakage current measured in this experiment.
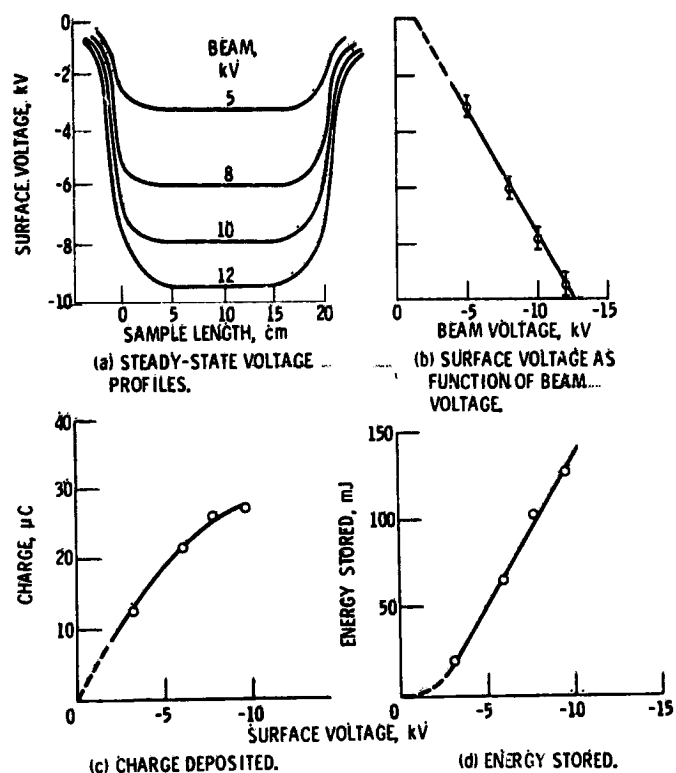
Figure 3.   Silver Teflon Charging Data

If the steady-state surface potential for the central portion of the sample is plotted against the beam voltage, a linear relationship results as shown in Figure 3(b). The surface voltage is simply 1800 V less than the beam voltage for the range shown. Since 1800 V is approximately the value for the secondary emission yield to be unity, the surface voltage appears to be controlled by the secondary emission; the leakage currents are too small to influence the surface potential.

If the leakage current transients are integrated, the charge deposited on the sample can be computed. A plot of this charge versus the central surface potential for each test condition is shown in Figure 3(c). The slope of this curve is the effective capacitance of the sample. This curve indicates that the capacitance depends upon the surface voltage. This effect is believed to be due to the edge effect on the surface voltage and not due to a change in the material dielectric coefficient.

Once the charge and surface potential are available, the energy stored in the sample can be computed. This result is shown in Figure 3(d).

436

3.2.2.2 Discharge Characteristics

When the beam voltage is increased above -12 kV, visible discharges occur similar to those shown in Figure 4. Pictured is a single discharge event as a result of bombardment with 20 keV electrons. Pinholes were deliberately placed in the center of each 5 cm width of tape. The discharges originate at the edges of the tape and the pinholes which are the places where the largest voltage gradients would be expected.
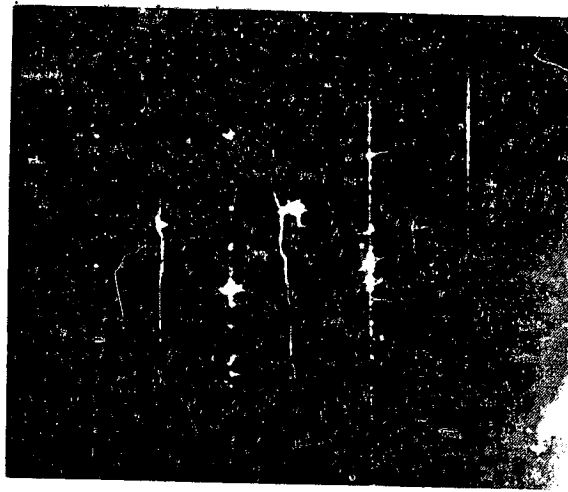
Figure 4. Discharges in Silver Teflon Sample.
Tape sample, conductive adhesive

The surface voltage and leakage current data obtained during a discharge test are shown in Figure 5.. The voltage probe was swept at discrete time intervals and the leakage current was recorded every minute. The actual time of the discharge was determined from the recorder trace of the leakage current. The charge deposited up to breakdown and the charge remaining on the sample after breakdown was computed by integrating the leakage current. The surface voltage was obtained from the probe readings. The energy lost was computed from the charge and voltage values. The effective value of the capacitance also computed from the charge and voltage values, was essentially a constant. The distinction between partial discharge and major discharge depends upon the charge and energy lost in the discharge; in a major discharge a large fraction of charge and stored energy is lost.

Typical characteristics for the discharges in silvered Teflon samples are summarized in Figure 6. One assumption made in these studies is that a single sweep across the sample provides a voltage profile representative of the entire
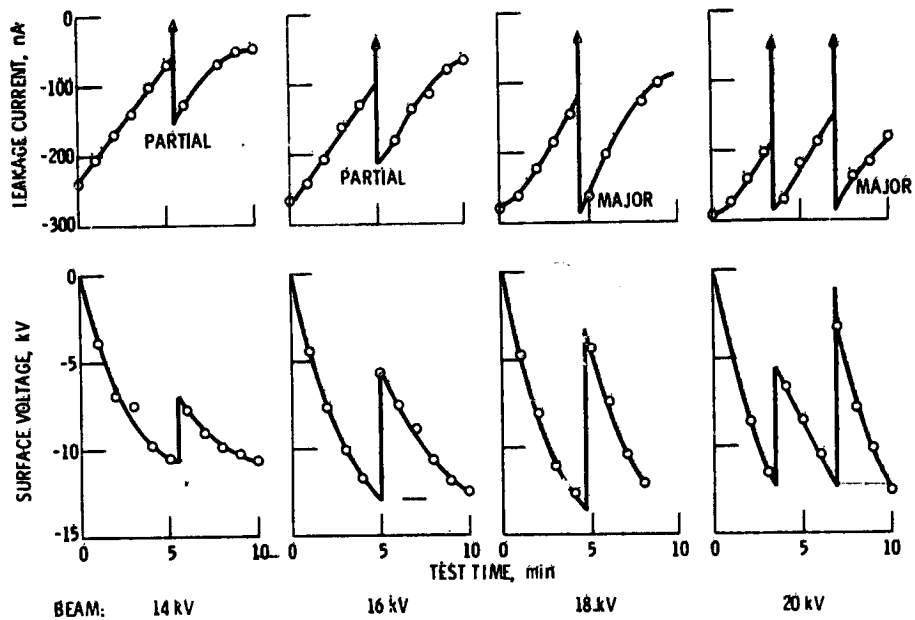
437

Figure 5. Discharge Characteristics of Silver Teflon Samples

AVERAGE DISCHARGE CHARACTERISTICS

VOLTAGE AT BREAKDOWN: -12 kV ±1.5 kV
CHARGE DEPOSITED: 50 µC ±10 µC
CHARGE LOST IN DISCHARGE: 20-60 µC
ENERGY IN DISCHARGE: 150-400 mJ

(a) VOLTAGE PROFILE - PARTIAL DISCHARGE.

(b) DISCHARGE CURRENT TRANSIENT - ELECTRON FLOW FROM GROUND TO SAMPLE.
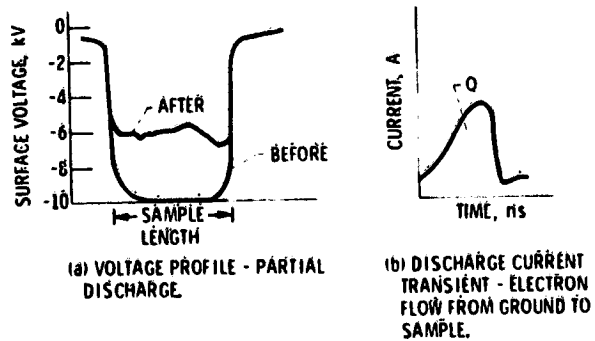
Figure 6. Discharge Characteristics of Silver Teflon Samples

438

sample. This assumption was verified by comparing sample surface potential profiles obtained just before and just after discharge with computed surface voltage values. These values were computed using a one-dimensional model for a silvered Teflon capacitor. These values are -10,700 V before discharge and -6500 V after discharge. These values are in good agreement with the actual probe readings of Figure 6(a). Hence, it appears that the voltage obtained from the probe sweep is representative of the whole sample.

The transient current pulses during a major discharge under 20 keV electron bombardment have also been obtained. A typical pulse is shown in Figure 6(b). The duration of this pulse is on the order of 500 nsec while the peak amplitude ranges between 20 and 100 A. The maximum values of charge represented by this pulse (from integration of the area under the curve) are on the order of 15 μC instead of the 50 to 60 μC of charge lost in discharge as computed from the surface voltage readings. The replacement current does not appear to compensate for all the charge that is lost in the discharge. A model of the discharge phenomenon is being developed.

As a result of the discharge tests there was some silver loss at the tape edges where the discharges originated. The loss was concentrated at the discharge location and did not appear to increase with time up to test times of several hours.

It was possible that the outgassing of the adhesive in the cracks between the tape might have influenced the discharging characteristics. To investigate this a test was conducted with a single sheet of silvered Teflon mounted on a wire frame with a minimal amount of adhesive on the sample back. Again the Teflon faced the electron beam. The silver layer was wired directly to the electrical ground. The test results were similar to those of the tape samples. The visible discharges observed under 20 keV electron bombardment are shown in Figure 7. This is a time exposure and represents about three major discharges. It appears that if there is any outgassing, it does not appreciably change the discharge characteristics.

3.3 Thermal Blanket Samples

3.3.1 SAMPLE DESCRIPTION

Four different types of Kapton outer layer blankets were evaluated in this series of tests. These samples are shown in Figure 8. Sample A, B, and D have 0.013 cm (5 mil) thick Kapton as the outer layer. Sample C has a 0.005 cm (2 mil) thick Kapton outer layer. Sample D has a sewn edge construction while the others have open edges. The interior portions of the blankets are 15 or 20 layers of aluminized Mylar. All metallic layers of all blankets were grounded through the electrometer. In all cases the samples were tested with the Kapton layer facing the electron source.
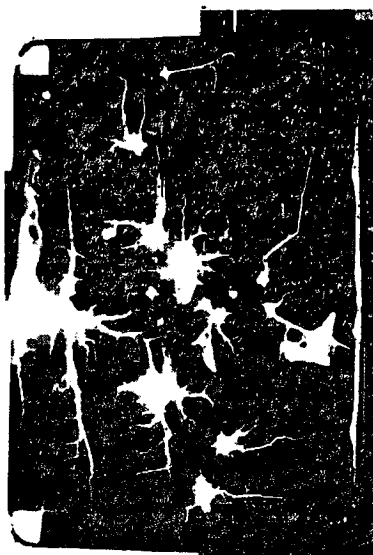
439

Figure 7. Discharges in Single
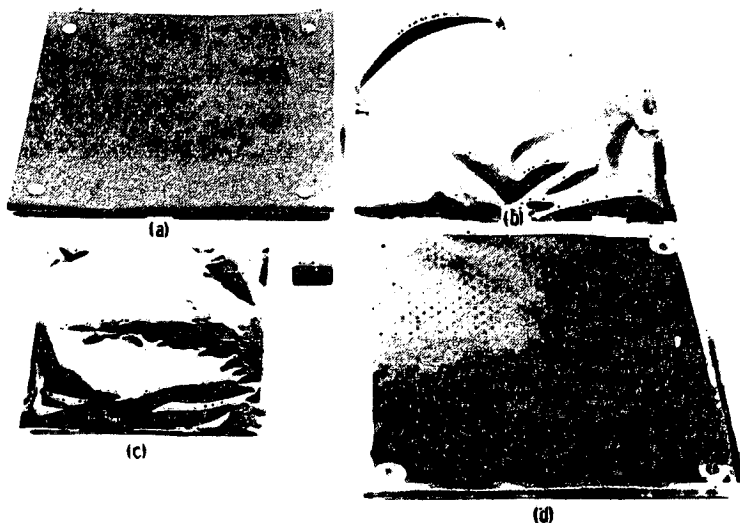Sheet Silver Teflon Sample _____

Figure 8. Kapton Thermal Blanket Samples

3.3.2 TEST RESULTS

3.3.2.1 Charging Characteristics

The charging characteristics are shown in Figure 9. The steady-state voltage profiles (Figure 9(a)) show the same characteristics as the silvered Teflon film: uniform potential across the central portion of the Kapton with very strong gradients at the edges. The distortion in the voltage profile at the right hand edge (above 5 kV beam voltage) occurred when the probe passed close to a blanket grounding tab.
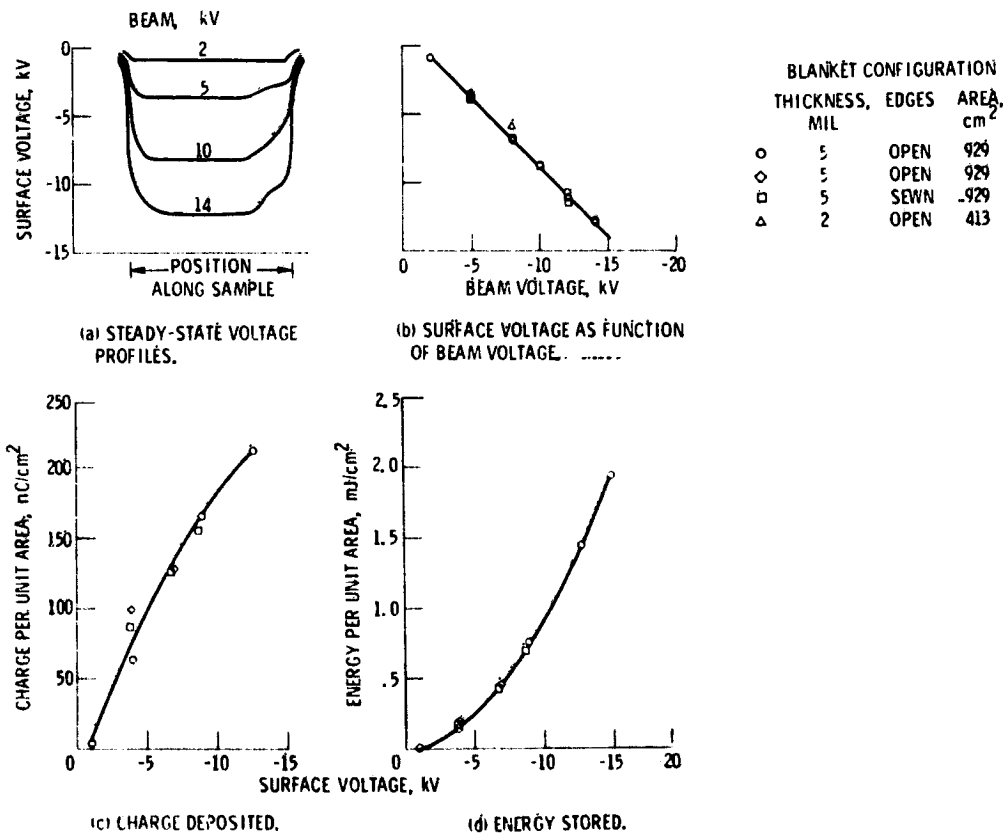

(a) STEADY-STATE VOLTAGE PROFILES.

(b) SURFACE VOLTAGE AS FUNCTION OF BEAM VOLTAGE. ......

	BLANKET CONFIGURATION		
	THICKNESS, MIL	EDGES	AREA, cm²
○	5	OPEN	929
◇	5	OPEN	929
□	5	SEWN	.929
△	2	OPEN	413

(c) CHARGE DEPOSITED.

(d) ENERGY STORED.

Figure 9

441

The plot of the steady-state voltage versus the beam voltage (Figure 9(b)) again shows a linear relationship for the 0.013 cm (5 mil) thick Kapton. The surface voltage for the Kapton is 1200 V less than the beam voltage, and again is controlled by the secondary emission characteristics of the surface. The 0.005 cm (2 mil) Kapton material begins with the surface voltage controlled by secondary emission. However, above -5 kV surface voltage, the effect of leakage current begins to slow the rise in surface voltage. This effect is expected based on the lower bulk resistance.

The charge deposited per unit surface area and the energy stored per unit surface area, are shown in Figure 9(c) and (d). The slope of the charge-surface voltage curve again changes with the voltage, showing that the capacitance varies with voltage. This variation is believed to be due to the voltage gradients at the material edges.

The conclusion from this work is that the charging characteristics of Kapton blankets do not appear to depend upon the method of edge treatment. The material thickness dependence is as anticipated. More pronounced effects of edge treatment will be discussed when discharge characteristics are reviewed.

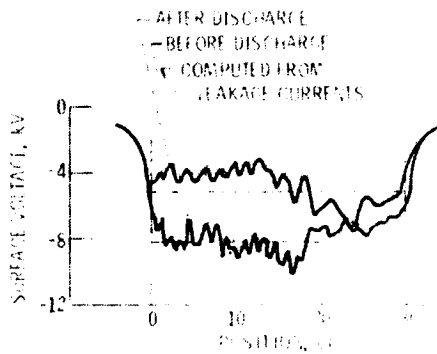### 3.3.2.2 Discharge Characteristics

The discharge characteristic data are shown in Figures 10 and 11. Generally, the discharge characteristics of the two 0.013 cm Kapton open edge blankets (Figures 8(a) and (b)) were similar. The 0.005 cm Kapton blanket and the sewn edge blankets (Figures 8(c) and (d)) behaved in a similar manner. Therefore, the discharge characteristics will be discussed only in terms of sewn edge blankets and open edge blankets.

The discharge characteristics of the sewn edge blankets are shown in Figure 10(a). In this figure the surface voltage probe traces just before and after discharge are displayed. Using the transient leakage current data to obtain values for the charge, and the computed value of the capacitance, the surface voltage has been calculated and superimposed on the voltage probe traces. The agreement is very good. Applying these techniques to all of the test data results in the breakdown characteristics listed. It has been found that the initial breakdown for each beam voltage test above -10 kV occurred when the average surface voltage was about -10.4 kV. After this initial breakdown subsequent discharges occurred when the average surface potential reached -8.2 kV. The energy dissipated in these discharges is relatively low. The number of discharges per unit test time, however, is fairly high.

The visible discharges observed on the sewn edge blanket are shown in Figure 10(b). The characteristic of the discharge is that of a glow of light over the Kapton surface with definite discharge spots at the thread line of the blanket edges. It is believed that this sewing acts as the trigger for the discharge.
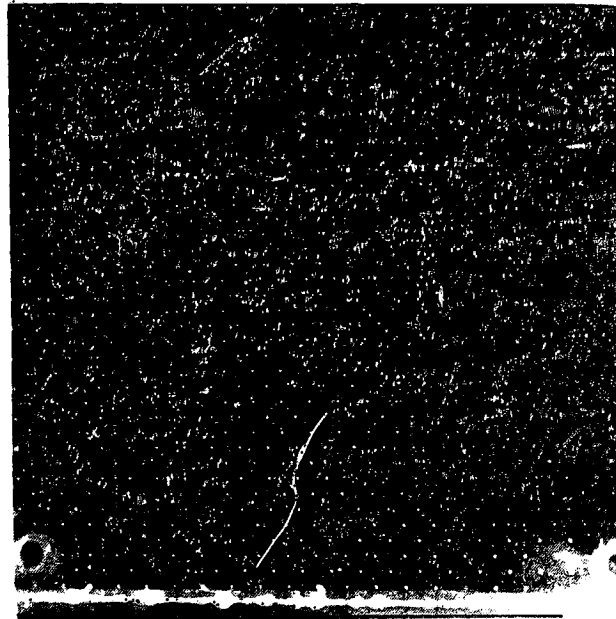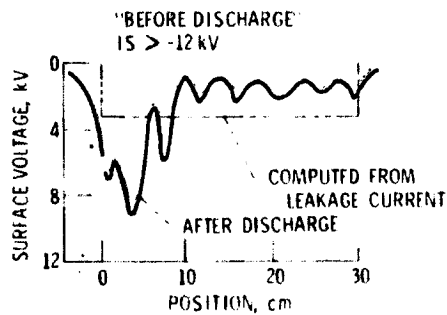
442

Figure 10. Discharge Characteristics of Sewn Edge Blanket

AVERAGE DISCHARGE CHARACTERISTICS

VOLTAGE AT BREAKDOWN:	-16.5 kV
CHARGE DEPOSITED:	250 μC
CHARGE LOST IN DISCHARGE:	200 μC
ENERGY IN DISCHARGE:	2.0 J

(a) Surface voltage profile.

Figure 11. Discharge Characteristics of Open Edge Blanket

443

The discharge characteristics of the open edge blankets are shown in Figure 11(a). Here, only the trace after the discharge has been obtained. The -12 kV limitation of the surface voltage probe prevented measuring the surface potential profile before discharges occurred. The agreement between the available voltage trace and computed average voltage is still good. As one can see from these characteristics, it requires a large voltage to cause the breakdown, but when it does discharge the energy dissipated is very large. Almost all of the stored energy in the blanket is lost. The visible discharges from this type of discharge are shown in Figure 11(b). The discharges appear as streaks originating at either vent holes or grounding points and extending across the blanket surface.

3.3.2.3 Effect of Sunlight on Kapton Blanket Characteristics

A sunlight-eclipse simulation test was conducted using an open edge, Kapton outer layer blanket (Figure 8(a)). The surface voltages measured during this test are shown in Figure 12. The conditions throughout this test were: -10 kV beam voltage with a 1 nA/cm^2 beam current density. The test was started with the sample potential at zero volts and then exposed to the electron flux with the solar simulator off. The sample charged to about -9 kV as expected. The effective resistance of the sample under the dark steady-state conditions was 3.6×10^{11} ohms.
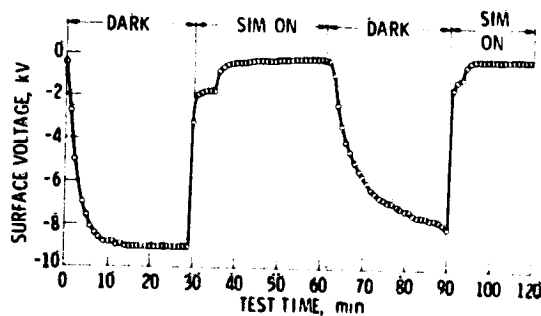

Figure 12. Effect of Sunlight on Kapton Thermal Blankets

The solar simulator was turned on 30 minutes after the test started and remained on for an additional 30 minutes. The surface voltage and the leakage current changed immediately (the step in the curve was cause by the two-stage turn on requirement of the solar simulator). After 30 minutes in the sunlight (at about 3/4 solar intensity), the surface voltage was decreased to about -200 V and the sample effective resistance reduced by 3 orders of magnitude (to 3.6×10^8 ohms).

444

At this point the simulator was turned off and the sample allowed to charge up again. The charging rate for thi eclipse cycle was slower than the first eclipse cycle. After the 30 minutes in the dark, the surface voltage reached only -7 kV corresponding to an effective resistance of 4×10^{10} ohms. Turning the solar simulator back on drove the the surface voltage back down to the -200 V level.

The test was repeated with the beam voltage set at 20 kV with a 1 nA/cm^2 beam current density. The initial dark eclipse simulation resulted in a series of discharges. When the simulator was turned on, the surface potential dropped again to about -200 V and all discharge activity ceased. After 20 minutes into the second eclipse simulation the potential was only about -6 kV with no discharge activity.

The behavior appears to be related to the photoconductivity effect reported for Kapton.[10] The Kapton material has shown an immediate decrease in bulk resistance with illumination and appears to slowly return to the original properties when returned to dark conditions. The Kapton behavior exhibited in these tests is probably not the result of photoemission from the sample since no other material tested with the solar simulator exhibited such an immediate and pronounced drop. The reduction in bulk resistivity could be enhanced by an increase in the sample temperature. But this should take a finite time to cause the change.

3.3.3 QUARTZ CLOTH OUTER LAYER BLANKET SAMPLES

Two samples of thermal blankets with Astroquartz cloth substituted for the Kapton outer layer were tested. One sample had a sewn edge (provided by Rockwell International, Inc.) while the second had open edges.

The test results are shown in Figure 13(a) and (b). The steady-state surface voltage as a function of beam voltage (Figure 13(a)) shows that the surface charges only to slightly more than -4 kV under a 20 kV beam test condition. The characteristic corresponds to a sample in which the resistance increases with the surface voltage. The sample effective resistance is shown in Figure 13(b). The transient leakage current data indicate that there is little, if any, charge stored in these samples.

There were no discharges observed during these tests. However, as with the S-13G paint sample, the blanket did electrofluoresce in the beam. A picture of the sample glowing is shown in Figure 14.

3.4 Solar Array Segments

3.4.1 SAMPLE DESCRIPTION

Three different solar array segments were evaluated in this test series. The segments are shown in Figure 15. Segment A is called the standard solar array segment. It is an array of 24 2- by 2-cm cells in series. The cells are 10 mils (0.025 cm) thick, 10 ohm-cm resistivity, N on P type solar cells. The cover
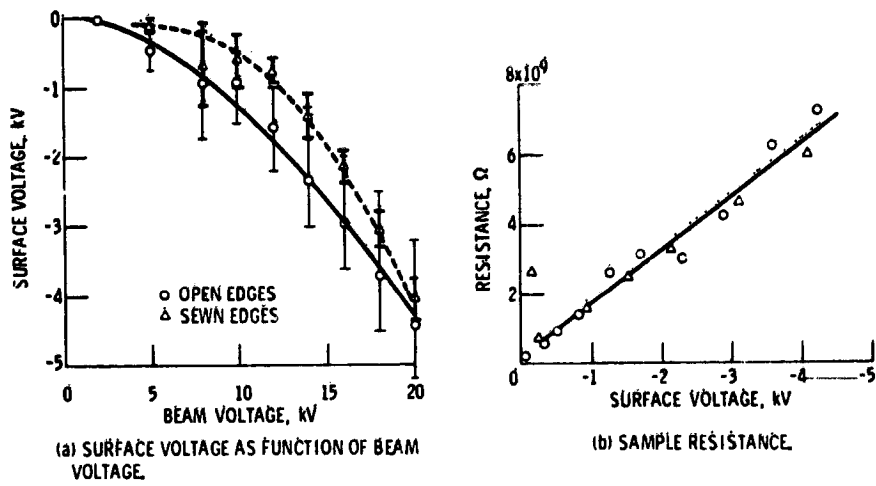
445

(a) SURFACE VOLTAGE AS FUNCTION OF BEAM VOLTAGE.

(b) SAMPLE RESISTANCE.

Figure 13. Quartz Cloth Thermal Blanket Charging Survey Data
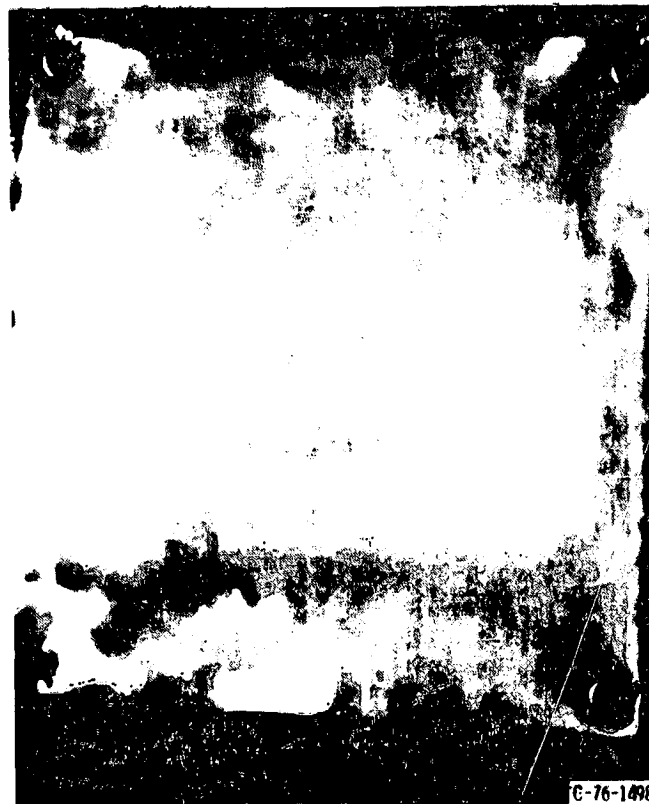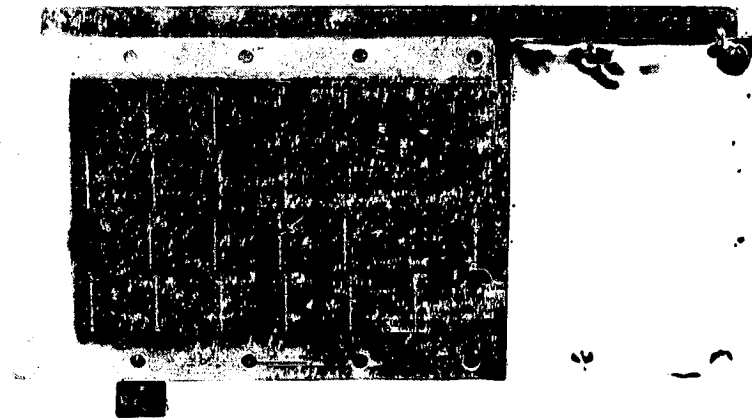

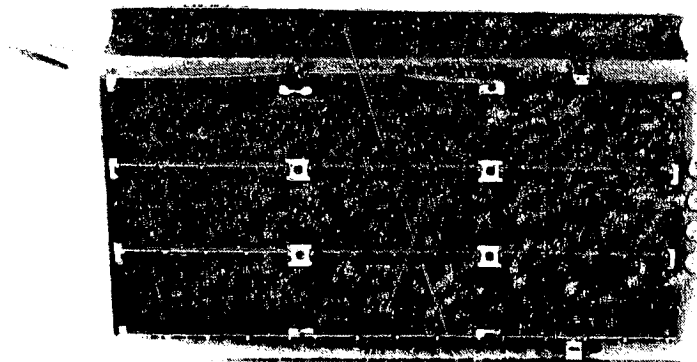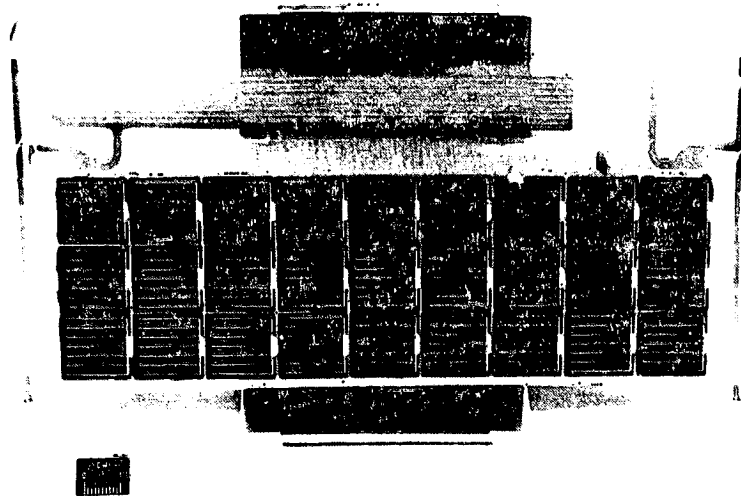Figure 14. Glow on Quartz Cloth Thermal Blanket

446

(a) Standard.

Figure 15

slides are 12 mils (0.03 cm) fused silica (Corning 7940). The cells are bonded to a Kapton sheet which is bonded to a fiberglass sheet. One end of the fiberglass board is covered with a grounded metal plate. The fibergla s on the other three edges of the segment is uncovered and exposed to the electron flux during the testing. The electrical circuit of the segment is grounded through the electrometer for the tests.

Segment B consists of 27 2- by 2-cm cells in a series/parallel configuration. These cells are mounted directly on a 3-mil (0.00"-cm) Kapton-fiberglass flexible substrate. The cells are 8-mil (0.012-cm) thick, 1 ohm-cm solar cells. The cover slides are 4-mil (0.006-cm) thick cerium doped microsheet. This segment has been constructed using the same techniques employed in manufacturing the Canadian-American Communications Technology Satellite array. [11]

Segment C consists of nine 2- by 4-cm cells in a series/parallel configuration with a conductive coating on the coverslides. These cells are mounted on a fiberglass board with about a 0.6 cm fiberglass border exposed at all four edges. The cells are 11-mil (0.028-cm) thick, 15 to 45 ohm-cm solar cells. The cover slides are 12-mil (0.03-cm) fused silica (Corning 7940) with a thin, transparent conductive coating applied by the Optical Coatings Laboratory (OCLI). The conductive coatings on each cell have been connected together at the four corners and electrically grounded. During the tests of this segment, the current collected by the conductive covers is monitored separately from the current collected by the array circuit.

3.4.2 TEST RESULTS

3.4.2.1 Charging Characteristics

The characteristics of the standard and flexible substrate segments (Figure 15(a) and (b)) are shown in Figures 16 and 17; the conductive coverslide segments will be discussed later. In Figure 16 the voltage profiles across the two segments are shown for various beam voltages. For both segments the effect of the edges is pronounced when the beam voltage exceeds -5 kV. The most severe voltage gradients are produced at the interface between the coverslides and the border. In fact, there is evidence that the border can control the charging of the coverslides (see Figure 16(a)). This effect suggests that material samples should be tested with the flight configuration boundaries in order to evaluate properly the behavior of any particular satellite exterior design.

The steady-state surface voltage reached by the coverslides and the substrates as a function of beam voltage, the charge deposited and energy stored in the segments are shown in Figure 17. The error bars on the voltage curves represent the range of values across the samples.
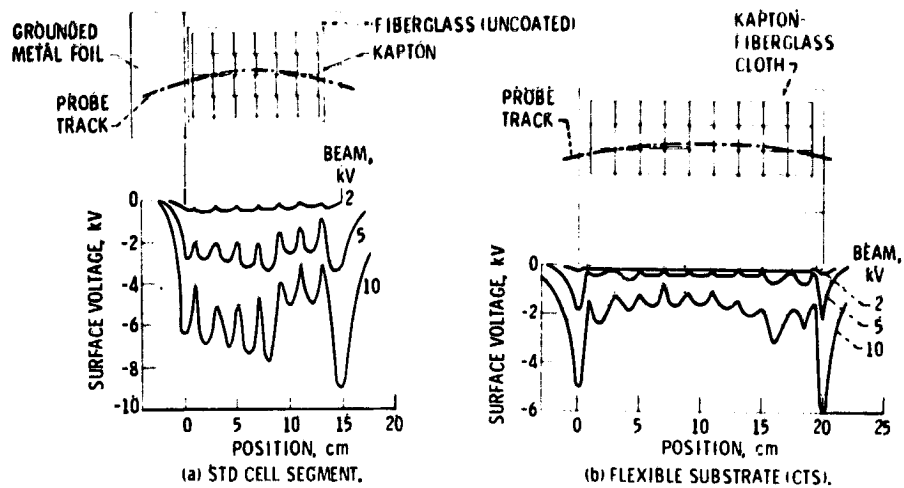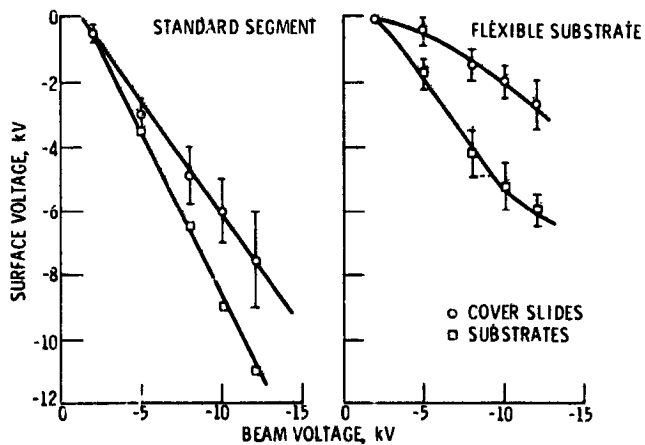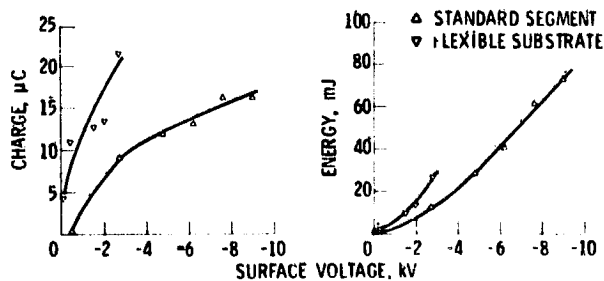
Figure 16

Figure 17

The surface voltage curve for the standard segment coverslide and the fiberglass are straight lines. This implies that the surface voltage for both is controlled by the secondary emission characteristics of each material with the fused silica being a slightly better emitter.

The surface voltage curve for the flexible substrate segment indicates that the cerium doped microsheet coverslides charge to a lesser value than the fused silica and behave as a material whose resistance increases with voltage. This behavior may be the result of the charging of the border and may not be real. This will be verified in future tests on the microsheet alone. The Kapton-fiberglass substrate behaves as expected. The surface voltage is controlled by secondary emission until the surface potential reaches about -9 kV at which point the leakage current influences the voltage and the curve starts to fall off.

The charge deposited on the coverslides of both segments, along with the energy stored, is shown in Figure 17(b) and (c) as a function of the coverslide average voltage. From these curves it is evident that, although the same charge is deposited on the flexible substrate segment as the standard segment, the energy stored in the flexible substrate segment is considerably less. This effect may be due to the charging of the substrate boundaries. In any case, the techniques used in constructing the flexible substrate segment appear to minimize the charging of the segment.

3.4.2.2 Discharging Characteristics

The discharge characteristics of only the standard array segment have been obtained. For this segment, discharges are observed when the beam voltage is about -14 kV. A picture of a typical discharge is shown in Figure 18. The discharges seem to originate at the edges of the coverslides and culminate in a flash of light over most of the coverslides. There is no apparent physical damage to the coverslides due to these discharges. The voltage-current characteristics of the segment are the same after this test as before. Long time discharge tests are planned to determine if the discharges can eventually decrease the array performance.

The discharge characteristics for this segment have been obtained from the leakage current measurements as shown in Figure 19. The charge stored is computed by integrating this current. The breakdown voltage is computed from the value of the capacitance and the computed charge deposited up to the point of discharge. The energy lost in the discharge is obtained by computing the energy stored at the time of the discharge and the energy remaining after the discharge. The average results for the three partial discharges and the 15 major discharges are tabulated on Figure 19. As can be seen the discharges seem to occur between -8 and -9 kV. In a partial discharge only about 25 mJ are lost whereas the full

450
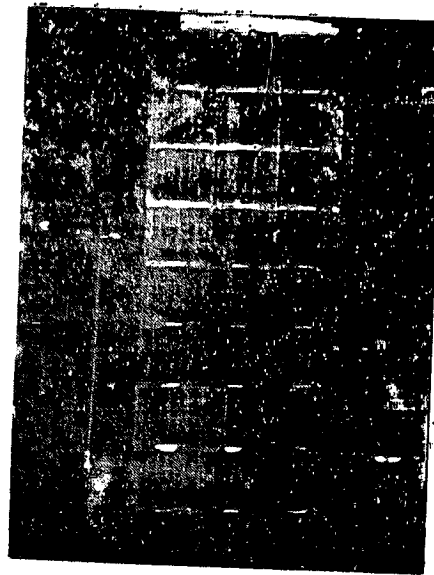
Figure 18. Discharges in Standard
Solar Array Segment

AVERAGE DISCHARGE CHARACTERISTICS

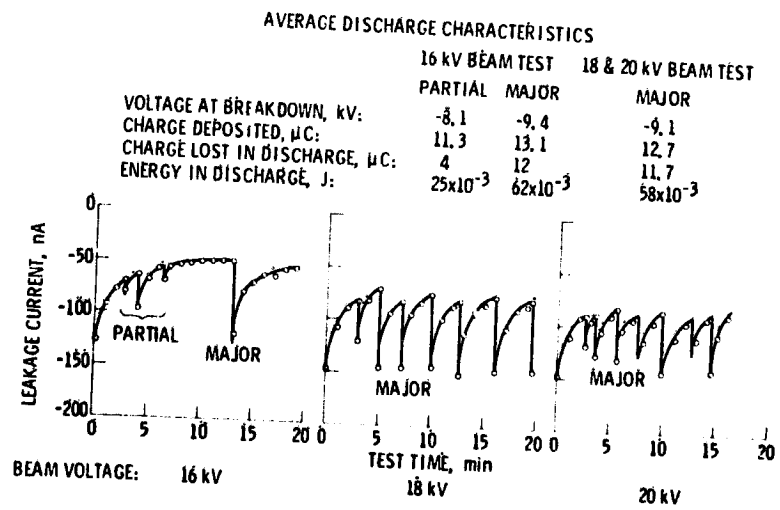|	16 kV BEAM TEST		18 & 20 kV BEAM TEST
	PARTIAL	MAJOR	MAJOR
VOLTAGE AT BREAKDOWN, kV:	-8.1	-9.4	-9.1
CHARGE DEPOSITED, μC:	11.3	13.1	12.7
CHARGE LOST IN DISCHARGE, μC:	4	12	11.7
ENERGY IN DISCHARGE, J:	25×10^{-3}	62×10^{-3}	58×10^{-3}

Figure 19. Discharge Characteristics of Standard Solar Array
Segment

60 mJ stored in the segment are lost in a major discharge. The reasons for partial discharges in some tests and major discharges in other tests are still to be established.

3.4.2.3 Effect of Solar Simulation on Flexible Substrate Segment

It is known that sunlight will increase the conduction in Kapton[10] exposed to the light. This increase would result in lowering the surface potential and possibly prevent discharging. However, there is a question of what would happen to the dark dielectric surfaces behind the solar cells if the array were exposed to a substorm condition while the cell side was illuminated. Would there be discharges? Or would the reduced resistivity of the illuminated Kapton affect the darkened areas? A test has been conducted at the LeRC to determine the response to these conditions. Additional testing of a similar array segment has been conducted in the ESTEC facility.[12]

The flexible substrate segment was mounted in the LeRC facility such that the dielectric side was exposed to the electron flux. A infrared, quartz arc lamp was mounted in the tank so that the light would illuminate the cell side of the segment at about 0.5 solar intensity. Test runs were made at several voltages at a beam current density of 10 nA/cm^2 first with the lamp off for 30 minutes, then with the lamp on for 30 minutes, followed by 60 minutes again in the dark and finally, 30 minutes with the lamp on again. The total number of discharges detected by the loop antenna 50 cm from the segment was counted at each beam current voltage. The results for the -10, -12, and -14 kV beam voltage tests are shown in Figure 20. Similar trends were found in the -16, -18, and -20 kV tests.

As is apparent from Figure 20, the segment experienced numerous discharges when the segment was in the dark initially. When the light was turned on the discharges stopped immediately. When the lamp was again turned off, the discharges occurred again, but at a significantly lower rate. Even the lower rate was terminated when the lamp was again turned on. Therefore, the light on the cell side of the segment seems to stop the discharges that occur when the dielectric side is bombarded with kilovolt electrons while the cell electrical circuit is grounded. The reason for this behavior is either due to the photoconductivity effect in Kapton or thermal effects in the dielectric (there was no attempt to control or measure the segment temperature during these tests).

The discharges that were observed during this test are shown in Figure 21. This picture is a multiple discharge exposure of the segment in the dark while the dielectric is bombarded. The majority of the discharges occur at the cell interconnects. This implies that the Kapton-fiberglass cloth is charged to a point where there is a breakdown through the cloth to the grounded interconnect. Preliminary calculations indicate that the surface potential is about -8 to -9 kV at the discharge
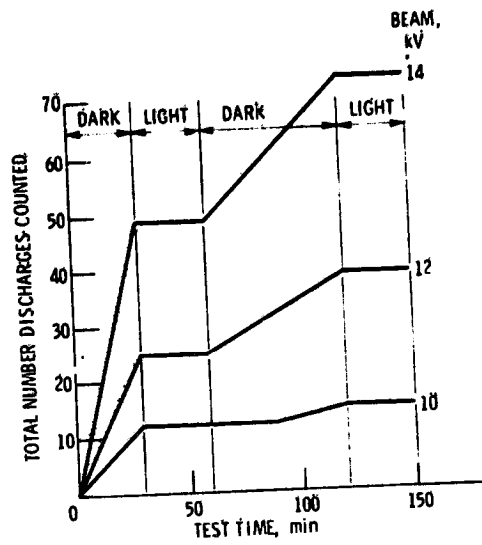
Figure 20. Discharge Characteristics. Eclipse simulation; flexible substrate segment, electron current density, 10 nA/cm^2
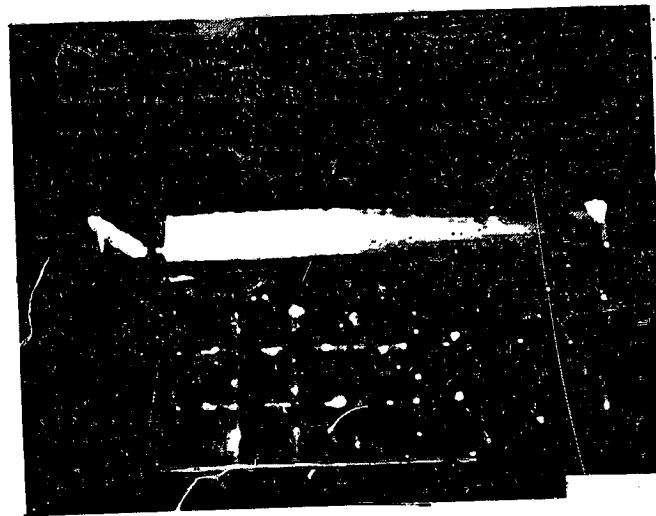

Figure 21. Discharges in Flexible Substrate Solar Array Segment

which is sufficient to break down the thin Kapton sheet between the fiberglass strands.

After running tests on the segment for about 40 hours, a marked decrease in the number of discharges was noted. The segment was removed from the facility and inspected. It was found that the cloth was punctured at every interconnect. This apparently reduced the number of discharges per unit time. There was no degradation of the cell characteristics as a result of these tests.

3.4.2.4 Conductive Coverslide Test Results

This segment was exposed only to a limited test. The voltage profiles obtained are shown in Figure 22. These profiles show that the conductive coverslides remained at ground potential while the surrounding fiberglass boundary charged to rather high potentials. In fact, these reached a point where discharges between the fiberglass and the thin conductive covers were possible. Therefore, the test was stopped. The fiberglass will be covered and grounded and the test will be repeated.
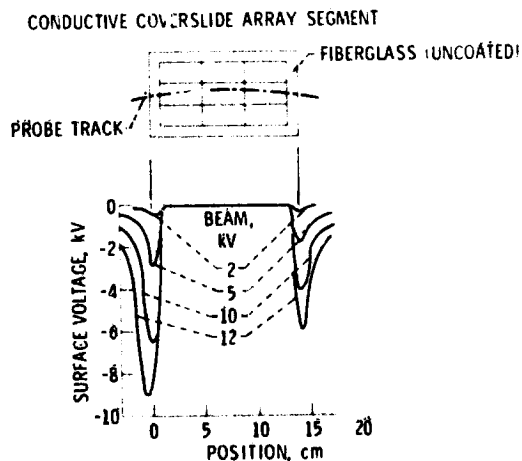

Figure 22. Steady-state Surface Voltage Profiles of Solar Array Segments

The conductive coverslides did collect currents proportional to the cell area and the beam current, as expected. There were no nonuniformities observed in the voltage profile over the conductive coverslides. The location of the gaps between the cells was barely discernible. The sample was very well behaved. The results again pointed out the need to test samples in flight configurations so that the effects of the surroundings can be evaluated.

4. CONCLUDING REMARKS

A series of survey tests have been conducted in the Lewis Research Center geomagnetic substorm simulation facility on typical spacecraft materials. The samples, ranging in size from 300 to 1000 cm^2 were exposed to monoenergetic electron energies from 2 to 20 keV at a current density of 1 nA/cm^2.

In general, all the insulator materials behave as if they were capacitors with one surface at ground potential while the surface facing the electron beam came to an equilibrium potential that depended upon the secondary emission, backscattering, and leakage currents. Strong voltage gradients were found at the edges of the samples and these must be considered in treating the sample as a simple capacitor. The effective capacitance of the sample appears to change with surface voltage as a result of this edge voltage gradient. Solar simulation changed the charging characteristics of the samples either because of photoemission, photoconduction, or thermal effects. Finally, it was found that the surroundings can influence the charging of the samples. Therefore, realistic evaluations of the behavior of materials for a specific design must include the effects of the surroundings in the flight configuration.

The samples in which discharges did not occur were the spacecraft paints (both conductive and nonconductive), quartz cloth samples and conductive coverslide solar array segments. In the case of the S-13G paint and the quartz cloth the samples were charged to limited voltage values, but they did "electrofluoresce" in the electron beam.

All of the other samples tested did discharge. The discharges normally originate at the sample edges or at imperfections on the surface. These are the places where the voltage gradients are the most severe. The discharges were visible and have been photographed. The discharges occurred when the surface potential was in the range of -8 to -12 kV. The energy lost in the discharges was computed to be in the range of about 0.6 mJ/cm^2 for the solar array segments to about 2 mJ/cm^2 for Kapton blankets. Construction techniques and surroundings were found to influence the discharge characteristics of the samples so that the evaluation for a particular spacecraft design should involve testing in flight configurations.

There are two scaling factors that still must be resolved. The first is the geometric scaling, or how to determine the characteristics of very large spacecraft surfaces from tests on small area samples. In order to obtain this scaling factor, large area tests in very large facilities must be conducted. Such a test. program is being considered for the near future.

The second scaling factor is the environmental scaling or the transition from monoenergetic electron fluxes to the distributed energy plasma of space. One attempt at this extrapolation is given in another paper of this session.[13] The final

answer will come only after space-flight data on the materials characteristics have been obtained from experiments such as those on SCATHA.[2]

The testing program that has been described here will continue until all of the significant parameters for the various spacecraft materials have been evaluated. The information gathered will be issued in reports and catalogued for incorporation in the Design Criteria Handbook that is to be the main output of the joint AF-NASA Spacecraft Charging Investigation.[4]

References

1. Fredricks, R. W., and Scarf, F. L. (1973) Observation of spacecraft charging effects in energetic plasma regions, in Photon and Particle Interactions with Surfaces in Space, R.J.L. Grard, Editor, D. Reidel Publishing Co., pp. 277-308.

2. McPherson, D. A., Cauffman, D. P., and Schober, W. (1976) Spacecraft charging at high altitudes: The Scatha satellite program, in Spacecraft Charging by Magnetospheric Plasmas. Progress in Astronautics and Aeronautics, Vol. 47, A. Rosen, Editor, Am. Inst. Aeronaut. Astronaut. / Mass. Inst. Tech., 1976, pp. 15-30.

3. Rosen, A. (1975) Spacecraft Charging — Environment Induced Anomalies, AIAA Paper 75-91, Pasadena, Calif.

4. Lovell, R. R., et al (1976) Spacecraft charging investigation: A joint research and technology program, in Spacecraft Charging by Magnetospheric Plasmas, Progress in Astronautics & Aeronautics, Vol. 47, A. Rosen, Editor, Am. Inst. Aeronaut. Astronaut./Mass. Inst. Tech., pp. 3-14.

5. Stevens, N.J., Lovell, R. R., and Gore, J. V. (1976) Spacecraft charging investigation for the CTS project, in Spacecraft Charging by Magnetospheric Plasmas, Progress in Astronautics & Aeronautics, Vol. 47, A. Rosen, Editor, Am. Inst. Aeronaut. Astronaut./Mass. Inst. Tech., pp. 263-275.

6. Berkopec, F. D., Stevens, N.J., and Sturman, J.C. (1976) The substorm simulation facility, Paper presented at the USAF/NASA Spacecraft Charging Technology Conference, Colorado Springs, Colo.

7. Stevens, N. J., Klinect, V. W., and Berkopec, F. D. (1976) Environmental Charging of Spacecraft Surfaces: Tests of Thermal Control Materials for use on the Global Positioning System Flight Space Vehicle. Part 1: Specimens 1-5, NASA TM X-73467.

8. Stevens, N. J., Berkopec, F. D., and Blech, R. A. (1976) Environmental Charging of Spacecraft Surfaces: Tests of Thermal Control Materials for use on the Global Positioning System Flight Space Vehicle. Part 2: Specimens 6-9, NASA TM X-73436.

9. Berkopec, F. D., and Stevens, N.J. (1976) Testing and evaluation of solar array segments in simulated geomagnetic substorm charging conditions, Paper presented at the 12th Photovoltaic Specialists Conference, Baton Rouge, La.

10. Coffey, H.T., Nanevicz, J.E., and Adamo, R.C. (1975) Photoconductivity of High-Voltage Space Insulating Materials, Stanford Research Inst., Menlo Park Calif.; also NASA CR-134995.

11. Buhs, R. (1974) Layout and technology of the CTS solar array blanket, in Conference Record on the 10th IEEE Photovoltaic Specialists Conference, Inst. Electri. Electron. Eng., New York, pp. 296-306.

12. Bogus, K.P. (1976) Investigation of a CTS solar cell test patch under simulated geomagnetic substorm charging conditions, Paper presented at the USAF/NASA Spacecraft Charging Technology Conference, Colorado Springs, Colo.

13. Purvis, C.K., Stevens, N.J., and Oglebay, J.C. (1976) Charging characteristics of materials:. Comparison of experimental results with a simple analytical model, Paper presented at the USAF/NASA Spacecraft Charging Technology Conference, Colorado Springs, Colo.